

PROCEEDINGS OF SPIE

SPIEDigitalLibrary.org/conference-proceedings-of-spie

Quantitative analysis of adipose tissue on chest CT to predict primary graft dysfunction in lung transplant recipients: a novel optimal biomarker approach

Yubing Tong, Jayaram K. Udupa, Chuang Wang, Caiyun Wu, Gargi Pednekar, et al.

Yubing Tong, Jayaram K. Udupa, Chuang Wang, Caiyun Wu, Gargi Pednekar, Michaela D. Restivo, David J. Lederer, Jason D. Christie, Drew A. Torigian, "Quantitative analysis of adipose tissue on chest CT to predict primary graft dysfunction in lung transplant recipients: a novel optimal biomarker approach," Proc. SPIE 10575, Medical Imaging 2018: Computer-Aided Diagnosis, 105753K (27 February 2018); doi: 10.1117/12.2294050

SPIE.

Event: SPIE Medical Imaging, 2018, Houston, Texas, United States

Quantitative Analysis of Adipose Tissue on Chest CT to Predict Primary Graft Dysfunction in Lung Transplant Recipients

– A Novel Optimal Biomarker Approach

Yubing Tong¹, Jayaram K. Udupa¹, Chuang Wang¹, Caiyun Wu¹, Gargi Pednekar¹,
Michaela D. Restivo^{3†}, David J. Lederer^{3†}, Jason D. Christie^{2†}, Drew A. Torigian¹

¹Medical Image Processing Group, Department of Radiology, University of Pennsylvania, Philadelphia, PA 19104; ²Division of Pulmonary and Critical Care Medicine, Hospital of the University of Pennsylvania Center for Clinical Epidemiology and Biostatistics, University of Pennsylvania School of Medicine, Philadelphia, PA 19104; ³Pulmonary & Intensive Care Translational Outcomes Research Group, Division of Pulmonary, Allergy, and Critical Care Medicine, Columbia University Medical Center, NY, 10032. [†]These authors contributed equally to this work.

ABSTRACT

In this study, patients who underwent lung transplantation are categorized into two groups of successful (positive) or failed (negative) transplantations according to primary graft dysfunction (PGD), i.e., acute lung injury within 72 hours of lung transplantation. Obesity or being underweight is associated with an increased risk of PGD. Adipose quantification and characterization via computed tomography (CT) imaging is an evolving topic of interest. However, very little research of PGD prediction using adipose quantity or characteristics derived from medical images has been performed.

The aim of this study is to explore image-based features of thoracic adipose tissue on pre-operative chest CT to distinguish between the above two groups of patients. 140 unenhanced chest CT images from three lung transplant centers (Columbia, Penn, and Duke) are included in this study. 124 patients are in the successful group and 16 in failure group. Chest CT slices at the T7 and T8 vertebral levels are captured to represent the thoracic fat burden by using a standardized anatomic space (SAS) approach. Fat (subcutaneous adipose tissue (SAT)/ visceral adipose tissue (VAT)) intensity and texture properties (1142 in total) for each patient are collected, and then an optimal feature set is selected to maximize feature independence and separation between the two groups. Leave-one-out and leave-ten-out cross-validation strategies are adopted to test the prediction ability based on those selected features all of which came from VAT texture properties. Accuracy of prediction (ACC), sensitivity (SEN), specificity (SPE), and area under the curve (AUC) of 0.87/0.97, 0.87/0.97, 0.88/1.00, and 0.88/0.99, respectively are achieved by the method. The optimal feature set includes only 5 features (also all from VAT), which might suggest that thoracic VAT plays a more important role than SAT in predicting PGD in lung transplant recipients.

Keywords: optimal biomarkers, feature extraction, lung transplantation, primary graft dysfunction (PGD), computed tomography (CT), adipose tissue.

1. INTRODUCTION

Primary graft dysfunction (PGD), a key parameter for liver, heart, and lung transplantation, is a syndrome encompassing a spectrum of mild to severe lung injury that occurs within the first 72 hours after lung transplantation [1-5]. PGD is also found to account for at least one third of deaths during the first post-operative month [6]. Recent research also shows that obesity or being underweight is associated with an increased risk of PGD [7-13]. Adipose tissue quantification via CT

imaging is an evolving topic of interest. However, very little research of PGD prediction using medical images has been performed to date.

The hypothesis of this study is that a feature-based approach, by using a small robust quantitative feature set derived from thoracic adipose tissue on pre-operative chest CT, is able to accurately distinguish patients who will develop PGD from those who will not develop PGD. We explore features related to thoracic adipose tissue on chest CT images to predict PGD. Two kinds of adipose tissues are usually considered in such analysis: subcutaneous adipose tissue (SAT) and visceral adipose tissue (VAT). Previous work showed that the area of fat (SAT or VAT) of a single slice optimally selected strongly correlates with 3D fat volumes in the thoracic and abdominal regions [14, 15], and the optimal slice can then be used to represent fat burden in the body regions.

In this study, patients who underwent lung transplantation are categorized into two groups of successful (positive) or failed (negative) transplantation according to PGD grade value at day 2 and day 3. The selected features from this study, which we call optimal biomarkers, can be separately computed and explained with their original meaning, which is impossible for the traditional dimensionality reduction approaches of feature selection such as principal component analysis. Those optimal features may be able to improve our understanding of the mechanism of PGD development and to predict development of PGD in the lung transplant setting.

2. METHOD

Image dataset

This image analysis study was conducted following approval from the Institutional Review Board at the University of Pennsylvania. Unenhanced CT image data sets from 140 adult lung transplant patients had been acquired as part of an NHLBI-funded and IRB-approved prospective study at 3 lung transplant centers: Columbia, Penn, and Duke. All participants provided informed consent. Chest scans were performed during full inspiration with multi-detector row CT scanners (Siemens Sensation, Definition, FLASH, and AS, Siemens Medical Systems; GE VCT & HD, General Electric) with 64 to 128 detector rows, 16 to 128 \times 0.6 to 1.25 mm slice collimation, kVp of 120, approximately 110-120 effective mAs for Siemens machines and 80-500 mA for GE machines with CareDose on, gantry rotation time of 0.4-0.5 s, reconstructed with I50f, B30, or B35 kernel for Siemens machines and Standard kernel for GE machines. The image size was 512 \times 512 with 50-70 slices, and the voxel size varied from 0.7 \times 0.7 \times 5 mm³ to 0.97 \times 0.97 \times 5 mm³.

Fat definition in 3D chest CT

For all samples in this study, thoracic body regions were defined consistently as extending from 15 mm superior to the apex of the lungs to 5 mm inferior to the base of the lungs. All patient CT images were accordingly trimmed to include just this standardized body region. In the inferior portion of the thorax, where axial slices pass through the curved diaphragm, abdominal visceral fat appears in the slices and has to be excluded. Generally, we define the thoracic SAT-VAT interface as the interior surface of the rib cage; fat within this surface is considered to be VAT and that external to this surface is defined as SAT for all slices which are superior to the diaphragm. For slices passing through the diaphragm, the definition of SAT remains the same. The VAT component, however, is modified in these slices by removing the visceral fat located within the abdomen. More details can be found in [14, 15]. Fat volume and area are computed by using the binary masks from image segmentation, which can be done manually by using the live wire tool in CAVASS software [16] or automatically by using the recently developed automatic anatomy recognition (AAR) approach [17] and then followed by morphology operations.

Once the binary masks have been obtained, it is important to normalize fat measurements of volume and area to account for variation in size of individual subjects. It may be expected that larger individuals will have overall larger solid organs and tissue regions. The factor of normalization employed was the length of the diagonal of a box that encloses thoracic skeleton, the idea being that the skeleton is a good indicator of the overall size of a subject. If L denotes this normalizing length for a subject, then fat volumes were normalized by dividing by L^3 , and fat areas were normalized by dividing by

L^2 . In general, both fat volume and area are normalized for executing the standardized anatomic space approach described in the following section.

Optimal slice derived from the standardized anatomic space (SAS) approach

The SAS approach, described in detail in [15], is landmark-based. It uses mid-axial levels of the vertebral bodies as landmarks in the cranio-caudal direction. Once defined, the landmarks are selected on 3D renditions of the skeletal structure. The approach consists of two stages - calibration and transformation. The purpose of calibration is to estimate mean locations of the landmarks, by using a few reference patient data sets. This stage is executed only once and not performed while analyzing each patient data set.

In the transformation stage, the same landmarks are identified on each patient image. A non-linear (piece-wise linear) mapping is defined between the patient landmarks and the estimated mean locations. This mapping defines the anatomic location of any given slice in the image data set of any patient in the standardized space. In other words, the mapping allows selecting the same anatomically “corresponding” or homologous slices in different patient studies by accounting for non-linearities that usually exist in the actual slice location relationships among patients. The SAS approach was used to identify the corresponding anatomic slices in each chest CT study, and SAT and VAT areas in each slice as well as their whole volumes were quantified. The ability of the slice at each anatomic location in the chest (and abdomen and thigh) to act as a marker of the measures derived from the whole chest volume was assessed via Pearson correlation coefficient (PCC) analysis. PCC between chest fat volume and chest slice fat area was maximal at the T8 level for SAT (0.97) and at the T7 level for VAT (0.86).

Deriving features

Based on the above consistent definition and delineation of thoracic adipose tissue, single chest CT slices at the T7 and T8 vertebral levels are captured to represent the fat burden (VAT and SAT, respectively) in the thoracic region by using the SAS approach. Due to the challenges in automatic or manual segmentation of 3D fat, feature extraction from a 2D optimal slice is much more convenient and efficient.

Features used in this study include fat tissue intensity properties and texture properties. Six texture properties are computed based on pixel intensity co-occurrence matrix including energy, entropy, maximum probability, contrast, inverse difference moment, and correlation [18]. Additional texture properties are derived using the local binary pattern (LBP) approach. Fat intensity properties, and texture properties from different texture computing parameters are collected to form a feature set consisting of 1142 features in total for each patient study.

Optimal biomarker selection and cross-validation strategy

The patients in this study are divided into two groups according to primary graft dysfunction (PGD) grade value at day two and day three after transplantation, which mainly indicates the failure or success of lung transplantation. PGD grade value 3 or greater at day 2 or 3 is considered to be a failure. The transplant should be considered as success otherwise. This resulted in 124 patients in the positive group (transplantation successful) and 16 in the negative group (transplantation failure). Optimal feature selection is then performed by using the OBM approach [19]. The idea of this approach is to find a small set of discriminating features from the large set of all features in several steps as follows:

- 1) Extract a subset of features that have a low level of correlation among all features. A heat map visualization technique that allows grouping of parameters based on correlations among them is used for this purpose.
- 2) Extract a subset of features from the whole set that is capable of separating the two patient groups of interest by using t-tests.
- 3) Find the intersection of the above two subsets to generate the final small feature set.

The accuracy of the selected features to perform classification of unseen images into the two patient groups was tested with leave-one-out and leave-ten-out strategies. Support vector machine (SVM) is used as the classifying engine. Due to

the sample imbalance of the two groups, for the training data set which is used for feature selection and training classifier, 50% of the positive groups and all negative samples are used for feature selection, and then another 50% of positive and all negative samples are used for training classifier. Testing data sets from the leave-one-out and leave-ten-out strategies have no intersection with the training data sets. Sensitivity, specificity, accuracy, and area under the ROC curve (AUC) are computed to describe the predictive performance of optimal feature sets consisting of different numbers of features.

3. RESULTS

In this study, fat (SAT/VAT) intensity properties, and texture properties based on LBP and co-occurrence matrix are assessed. Co-occurrence matrix-based properties are calculated with different window sizes including 3×3 , 5×5 , and 7×7 , different depth, and all orientations (in 360 degrees). Figure 1 shows the optimal single slices at T8 (for SAT) and T7 (for VAT) and corresponding masks of SAT/VAT on chest CT images for two patients who belong to the two groups considered (left: failure group, right: successful group). The corresponding texture images derived from the texture property “energy” with a window size of 5×5 are also displayed.

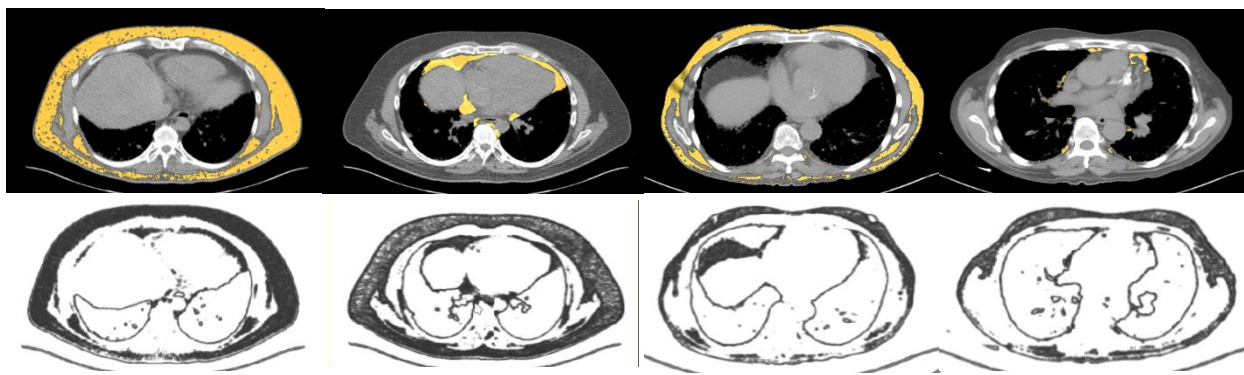


Fig. 1. SAT and VAT masks and texture images for two patients. The left two columns are for a failure group patient (PGD = 3) with SAT and VAT components marked in yellow in the top row and corresponding texture images in the bottom row. The right two columns are for a successful group patient (PGD = 0).

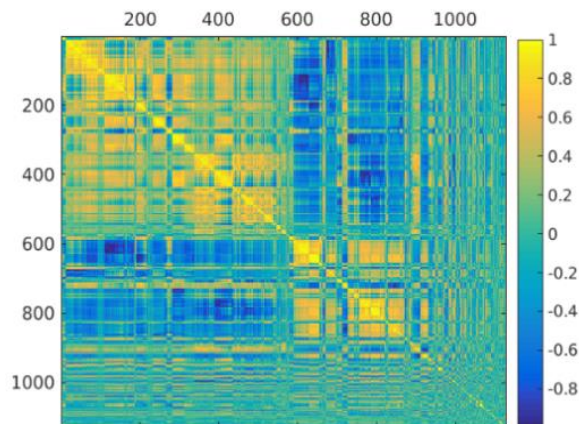


Fig.2 Correlation matrix of all features.

Figure 2 displays the correlation matrix for all features by using a heat map method of visualization. The size of the optimal feature set is within our choice and varies for a given level of accuracy according to the feature selection parameters [9]. In this study, we selected optimal feature sets with 5 features. The key point here is not to find as many features as possible but to find a small size and useful feature set to distinguish between the two groups with as high accuracy as possible. Table 1 lists the corresponding performance measures by using the accuracy of prediction (ACC), sensitivity (SEN), specificity (SPE), and area under the curve (AUC) and two validation strategies.

Table 1. OBM performance with 5 features.					
Cross-validation	Number of features	ACC	SEN	SPE	AUC
Leave-one-out	5	0.87	0.87	0.88	0.88
Leave-ten-out	5	0.97	0.97	1.00	0.99

The optimal feature set with only 5 features from VAT achieves ACC, SEN, SPE, and AUC of 0.87, 0.87, 0.88, and 0.88, respectively, by using the leave-one-out strategy. This level of performance with a small number of features is, we believe, excellent. The resulting 5 features are: 4th moment, kurtosis, skewness for *energy* with a window size of 7×7 ; peak height for *correlation* with a window size of 5×5 ; and skewness for *maximum probability* with a window size of 7×7 .

4. CONCLUSIONS

This is the first study to demonstrate highly accurate prediction of PGD via chest CT images acquired pre-operatively in patients who underwent lung transplantation. The derived features performed well with different validation strategies. Across all optimal feature sets, all features are from among texture properties. Properties derived from CT intensity (Hounsfield) distributions do not seem to be capable of separating/predicting the two groups. All optimal features found are VAT specific. Like intensity features, SAT-specific features also do not have predictive power.

The proposed method may offer a real practical means of predicting primary graft dysfunction by performing a single CT slice acquisition at the mid T7 level, segmenting VAT in this slice, and quantifying the optimal VAT-specific texture properties found in this investigation. Such an analysis performed on both lung transplant donors and recipients may shed further light on the role of both in the success of lung transplant surgery. This is clinically a highly practical method. Larger studies need to be conducted in the future in this fashion of single slice measurement to independently validate the findings of this paper.

Acknowledgements

This research is partly funded by DHHS grant R01 HL114626 (Lederer/Christie), R01 HL087115 (Christie), K24 HL115354 (Christie), and K24 HL131937 (Lederer).

References

- [1] Fernandez-Merino FJ, Nuno-Garza J, Lopez-Hervas P, Lopez-Buenadicha A, Moreno-Caparros A, Quijano-Collazo Y, Sanjuanbenito A, Vicente-Lopez E. Impact of donor, recipient, and graft features on the development of primary dysfunction in liver transplants. *Transplant Proc.* 2003;35(5):1793-4. PubMed PMID: 12962797.
- [2] Aharinejad S, Andrukhova O, Gmeiner M, Thomas A, Aliabadi A, Zuckermann A, Krenn K, Grimm M. Donor serum SMARCAL1 concentrations predict primary graft dysfunction in cardiac transplantation. *Circulation.* 2009;120(11 Suppl):S198-205. doi: 10.1161/CIRCULATIONAHA.108.842971. PubMed PMID: 19752368.
- [3] Szarszoi O, Besik J, Smetana M, Maly J, Urban M, Maluskova J, Lodererova A, Hoskova L, Tucanova Z, Pirk J, Netuka I. Biomarkers of cellular apoptosis and necrosis in donor myocardium are not predictive of primary graft dysfunction. *Physiol Res.* 2016;65(2):251-7. PubMed PMID: 26447521.
- [4] Porteous MK, Diamond JM, Christie JD. Primary graft dysfunction: lessons learned about the first 72 h after lung transplantation. *Curr Opin Organ Transplant.* 2015;20(5):506-14. doi: 10.1097/MOT.0000000000000232. PubMed PMID: 26262465; PMCID: PMC4624097.
- [5] Suzuki Y, Cantu E, Christie JD. Primary graft dysfunction. *Semin Respir Crit Care Med.* 2013;34(3):305-19. doi: 10.1055/s-0033-1348474. PubMed PMID: 23821506; PMCID: PMC3968688.
- [6] Olland A, Reeb J, Leclercq A, Renaud-Picard B, Falcoz PE, Kessler R, Schini-Kerth V, Kessler L, Toti F, Massard G. Microparticles: A new insight into lung primary graft dysfunction? *Hum Immunol.* 2016;77(11):1101-7. doi: 10.1016/j.humimm.2016.07.001. PubMed PMID: 27381358.

- [7] Gonzalez-Fernandez C, Gonzalez Castro A, Diaz-Reganon G. [Fatal donor-acquired fat embolism syndrome leading to multiple organ failure in a lung transplant recipient]. *Arch Bronconeumol*. 2009;45(9):469-70. doi: 10.1016/j.arbres.2008.10.007. PubMed PMID: 19410351.
- [8] Kyle UG, Genton L, Mentha G, Nicod L, Slosman DO, Pichard C. Reliable bioelectrical impedance analysis estimate of fat-free mass in liver, lung, and heart transplant patients. *JPEN J Parenter Enteral Nutr*. 2001;25(2):45-51. doi: 10.1177/014860710102500245. PubMed PMID: 11284469.
- [9] Day JD, Walden SM, Stuart SR, Hutchins GM, Hruban RH. Fatal fat embolism syndrome after numerous vertebral body compression fractures in a lung transplant recipient. *J Heart Lung Transplant*. 1994;13(5):785-90. PubMed PMID: 7803419.
- [10] Bozso SJ, Nagendran J, Gill RS, Freed DH, Nagendran J. Impact of Obesity on Heart and Lung Transplantation: Does Pre-Transplant Obesity Affect Outcomes? *Transplant Proc*. 2017;49(2):344-7. doi: 10.1016/j.transproceed.2016.12.002. PubMed PMID: 28219596.
- [11] Lederer DJ, Kawut SM, Wickersham N, Winterbottom C, Bhorade S, Palmer SM, Lee J, Diamond JM, Wille KM, Weinacker A, Lama VN, Crespo M, Orens JB, Sonett JR, Arcasoy SM, Ware LB, Christie JD, Lung Transplant Outcomes G. Obesity and primary graft dysfunction after lung transplantation: the Lung Transplant Outcomes Group Obesity Study. *Am J Respir Crit Care Med*. 2011;184(9):1055-61. doi: 10.1164/rccm.201104-0728OC. PubMed PMID: 21799077; PMCID: PMC3208644.
- [12] Lederer DJ, Wilt JS, D'Ovidio F, Bacchetta MD, Shah L, Ravichandran S, Lenoir J, Klein B, Sonett JR, Arcasoy SM. Obesity and underweight are associated with an increased risk of death after lung transplantation. *Am J Respir Crit Care Med*. 2009;180(9):887-95. doi: 10.1164/rccm.200903-0425OC. PubMed PMID: 19608717; PMCID: PMC2773915.
- [13] Upala S, Panichsillapakit T, Wijarnpreecha K, Jaruvongvanich V, Sanguankeo A. Underweight and obesity increase the risk of mortality after lung transplantation: a systematic review and meta-analysis. *Transpl Int*. 2016;29(3):285-96. doi: 10.1111/tri.12721. PubMed PMID: 26613209.
- [14] Tong Y, Udupa JK, Torigian DA, Odhner D, Wu C, Pednekar G, Palmer S, Rozenshtein A, Shirk MA, Newell JD, Porteous M, Diamond JM, Christie JD, Lederer DJ. Chest Fat Quantification via CT Based on Standardized Anatomy Space in Adult Lung Transplant Candidates. *PLoS One*. 2017;12(1):e0168932. doi: 10.1371/journal.pone.0168932. PubMed PMID: 28046024; PMCID: PMC5207652.
- [15] Tong Y, Udupa JK, Sin S, Liu Z, Wileyto EP, Torigian DA, Arens R. MR Image Analytics to Characterize the Upper Airway Structure in Obese Children with Obstructive Sleep Apnea Syndrome. *PLoS One*. 2016;11(8):e0159327. doi: 10.1371/journal.pone.0159327. PubMed PMID: 27487240; PMCID: PMC4972248.
- [16] Grevera G, Udupa JK, Odhner D, Zhuge Y, Souza A, Iwanaga T, et al. CAVASS: a computer-assisted visualization and analysis software system. *Journal of digital imaging*. 2007; 20 Suppl 1:101-18.
- [17] Udupa JK, Odhner D, Zhao L, Tong Y, Matsumoto MM, Ciesielski KC, et al. Body-wide hierarchical fuzzy modeling, recognition, and delineation of anatomy in medical images. *Med Image Anal*. 2014; 18(5):752-771.
- [18] Sonka M, Hlavac V, Boyle R. *Image Processing, Analysis, and Machine Vision*, Chapter 3.2.10, Principal Component Analysis, 74-77, 4th ed. Cengage Learning, 2015. ISBN-13: 978-133-59360-7.
- [19] Tong Y, Udupa JK, Torigian DA. Optimization of abdominal fat quantification on CT imaging through use of standardized anatomic space: a novel approach. *Med Phys*. 2014;41(6):063501. doi: 10.1118/1.4876275. PubMed PMID: 24877839; PMCID: PMC4032419.